Infrared Spectroscopy of Small Sodium-Doped Water Clusters: Interaction with the Solvated Electron†

Udo Buck*

Max-Planck-Institut für Dynamik und Selbstorganisation, Bunsenstrasse 10, D-37073 Göttingen, Germany

Ingo Dauster

Institut für Physikalische Chemie, Universität Göttingen, Tammannstrasse 6, D-37077 Göttingen, Germany

Bing Gao and Zhi-feng Liu

Department of Chemistry and Centre for Scientific Modeling and Computation, Chinese University of Hong Kong, Shatin, Hong Kong, China

Received: July 20, 2007; In Final Form: September 13, 2007

The measured vibrational OH-stretch spectra of size-selected $Na(H_2O)_n$ clusters for $n = 8$, 10, 16, and 20 are compared with first-principle calculations, which account for the interaction of the sodium cation, the electron, and the water molecules with the hydrogen-bonded network. The calculated harmonic frequencies are corrected by comparing similar results obtained for pure water clusters with experiment. The experimental spectra are dominated by intensity peaks between 3350 and 3550 cm^{-1}, which result from the interaction of the H atoms with the delocalized electron cloud. The calculations, which are all based upon the average spectra of the four lowest-energy isomers, indicate that most of the peaks at the lower end of this range (3217 cm^{-1} for $n = 8$) originate from the interaction of one H atom with the electron distribution in a configuration with a single hydrogen-bonding acceptor. Those at the upper end (3563 cm^{-1} for $n = 8$) come from similar interactions with two acceptors. The doublets, which arise from the interaction of both H atoms with the electron, appear in the red-shifted part of the spectrum. They are with 3369/3443 cm^{-1} quite pronounced for $n = 8$ but slowly vanish for the larger clusters where they mix with the other spectral interactions of the hydrogen-bonded network, namely, the fingerprints of the free, the double, and the single donor OH positions known from pure water cluster spectroscopy. For all investigated sizes, the electron is sitting at the surface of the clusters.

I. Introduction

The solvated electron in liquid solutions, although known for many years, is still an object of ongoing research.[1] The interaction of the excess electron with the solvent molecules is treated from the dielectric continuum[2] and semicontinuum models[3] to a full treatment of the dynamics using quantum path integral and local density functional methods.[4−8] In the course of these investigations, large clusters were also treated in a similar way[9−11] in order to interpret corresponding experiments of anionic water[12,13] and ammonia[14] clusters. Recently, the advent of a new series of experiments on anionic water clusters[15−18] has solicited also new theoretical investigations,[19] mainly on the question of the position of the electron which goes either inside of the cluster beyond a certain size or stays at the surface of the clusters. In the photodetachment experiment of clusters up to $n = 200$, Verlet et al.[17] observed different kinds of isomers with different electron vertical binding energies, which they attribute to surface and interior sites. The different behavior starts at around $n = 11$. This was called into question by a recent theoretical investigation on a series of properties of anionic water clusters by Turi and co-workers.[19] They claim that all experimental data available are in agreement with the assignment of surface-bound electronic states. The transition to interior states occurs at much larger sizes. The vibrational predissociation spectra in the size ranges of $n = 4−6$ (ref 15) and $n = 6−21$ (ref 16) in the region of the OH stretch clearly show fingerprints of the direct interaction of the water molecules with the electron distribution. Here, a very pronounced doublet is observed, which is attributed to the interaction of the two H atoms of a water molecule in a double acceptor (AA) position. The motif gradually shifts to smaller frequencies and disappears around $n = 11$.

Experiments on neutral clusters, which also reflect the behavior of the solvated electron, are mainly concentrated on the measurement of ionization potentials (IP).[20,21] Very recently, the first experiments on the infrared spectra in the OH-stretch region of size-selected $Na(H_2O)_n$ clusters in the size range from $n = 8$ to 60 were published.[22] The size selection was achieved by coupling the UV radiation of a dye laser below the threshold for ionization with the tunable IR radiation of an optical parametric oscillator. A different approach, namely, depletion spectroscopy, has been applied in the measurement of the IR spectroscopy of $Li(NH_3)_n$ for $n = 4−7$.[23] At the same time, new calculations became available on the ionization-induced relaxation in $Na(H_2O)_n$ and $Na(NH_3)_n$ clusters.[24] Here, the solute−solvent ($Na^+−H_2O$), the solvent−solvent ($H_2O−H_2O$), and the electron−solvent interactions were taken into account. The size range covered included $n = 4−8$, 10, 16, and 20 for the water system and $n = 4−11$ for the ammonia system.

† Part of the "Giacinto Scoles Festschrift".

* To whom correspondence should be addressed. E-mail: ubuck@gwdg.de.

10.1021/jp075717o CCC: $37.00
Published on Web 11/15/2007

In the present contribution, we compare the measurements of the IR spectra of $Na(H_2O)_n$ clusters for $n = 8$, 10, 16, and 20 with calculations of the same spectra based on the structures of ref 24. For this purpose, the results of the harmonic calculations of the frequencies were corrected by the comparison of the experimental results of water clusters[25] with calculations of the same kind and the same basis sets. In this way, we obtained information about the structure of the clusters and the binding sites to the electron. In addition, we compare the results for $Na(H_2O)_{20}$ with the calculated results for $(H_2O)_{20}$ (ref 26) and $Na^+(H_2O)_{20}$ (ref 27) and the experiments on $(H_2O)_{20}^-$.[16] Experiments with solvated alkali ions are available for $Cs^+(H_2O)_n$ but only up to sizes of $n = 5$.[28]

II. Experimental Section

The experiments were carried out in a molecular beam machine, which has been described in detail elsewhere.[29] Therefore, we will present here only a short account of the main parts, with emphasis on those that have been changed. The machine consists of a source chamber, a buffer chamber, and a detector unit. In a first step, the water clusters are produced by expanding water vapor of 0.53 bar seeded in helium at 4 bar through a nozzle of conical shape with a diameter of 63 μm, an opening angle of 41°, and a length of 2 mm. These clusters are doped by a single sodium atom by passing the beam through a pick-up cell, which is placed in the buffer chamber and kept at a pressure of 0.023 mbar. The clusters are detected by a reflectron time-of-flight mass spectrometer. Under optimal conditions, a mass resolution of $m/\Delta m = 1600$ is obtained at $m = 200$ u, based on the drift length of 1820 mm. The ions are extracted in the direction of the beam and detected on a microsphere plate. The mass spectra are sampled using a digital storage oscilloscope in a special particle counting mode. The spectra are corrected for the size dependence of the detection probability and the ionization cross section, the transformation from time to mass coordinates, and double ionization processes. The average size of the $Na(H_2O)_n$ clusters was measured to be $\langle n \rangle = 30$ under the above-mentioned source conditions.

The ionization is carried out in double resonance by the photons of a dye laser pumped by an excimer laser with a pulse width of 28 ns and the IR photons. The UV laser operates with 400 nm, which turned out to give the optimal signal enhancement for the product ions.[22] The infrared radiation used to excite the clusters is obtained from a Nd:YAG-laser-pumped optical parametric oscillator (OPO) in the spectral range from 2900 to 3800 cm^{-1}.[30,31] It consists of a master oscillator containing a $LiNbO_3$ crystal, which is pumped by the fundamental of a Nd:YAG laser. The master oscillator is seeded by the narrow-bandwidth infrared radiation obtained by difference frequency mixing the output of a pulsed dye laser and the 532 nm radiation of the same Nd:YAG laser in a $LiIO_3$ crystal. The typical output energy for the low-frequency component (idler) is ≥ 4 mJ per pulse in the entire spectral range covered in this study. The pulse width is 10 ns. The bandwidth of the infrared radiation, which is determined by the bandwidth of the dye laser, is chosen to be 0.5 cm^{-1}. We note that the wavenumber region between 3480 and 3510 cm^{-1} cannot be reached in the experiment caused by water impurities in the crystal. The time synchronization of the two laser beams is achieved by triggering the IR laser by a pulse delay generator. The UV pulse of the second laser is time delayed by about 80 ns with respect to the IR laser. This value is adjusted by optimizing the enhancement signal.

The results for the selected cluster sizes $n = 8$, 10, 16, and 20 are presented in Figure 1. All spectra are dominated by the peaks around 3400−3600 cm^{-1}. They agree in the two smaller peaks at 3640 and 3725 cm^{-1}. At the other end of the spectrum between 3000 and 3300 cm^{-1}, several more or less pronounced peaks appear, which differ in their positions and intensity for the different sizes. In general, the intensity increases in this frequency range with increasing cluster size.

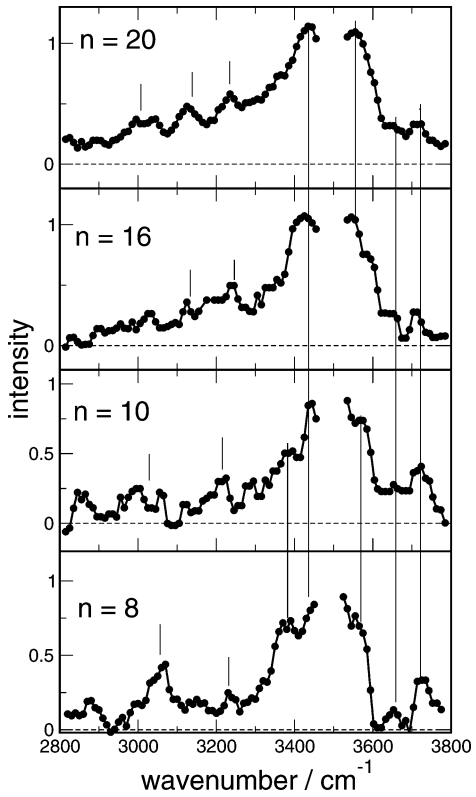

Figure 1. Measured OH-stretch spectrum of selected $Na(H_2O)_n$ clusters for the sizes indicated. The lines mark possible transitions at similar or different positions.

III. Calculations

A. Applied Methods. The details of the computational methods to sample the structures of $Na(H_2O)_n$ and $Na(NH_3)_n$ have been reported in a previous report.[24] Briefly, these structures are produced in two steps. In the first step, a density functional theory based ab initio molecular dynamics (AIMD) method is employed to sample representative structures at finite temperatures. Such a step is necessary due to the numerous isomers with similar energies and the low transition barriers between these isomers. AIMD simulations are performed at 300 K for $Na(H_2O)_n$ and at 200 K for $Na(NH_3)_n$, using the VASP[32−35] program with standard setup.[24] Structures systematically selected out of these AIMD simulations are then used in the second step as the starting geometries for structural optimizations at the B3LYP/6-31+G** level using the Gaussian program.[36] Structures at a specific size are ranked according to their energies. Harmonic frequencies are calculated for all of these structures, both to provide comparisons with experiments and to verify that there are no imaginary vibrational frequencies.

In the further course of this paper, we will describe the type of bonding of the water molecules by the behavior of the H atom. If the H is hydrogen bonded to the O atom of another water molecule, it is called a donor (D), and if the O atom receives a hydrogen bond, it is called an acceptor (A). In the case of the direct interaction of the H atoms with the electron cloud, the D is replaced by e, and the direct coordinations of

TABLE 1: Comparison of Experimental and Calculated Frequencies for Water Clusters in cm^{-1}

n	mode	calculation	experiment	factor
3	free	3894	3726	0.957
4	free	3884	3714	0.956
5	free	3888	3714	0.955
8	free	3885	3727	0.959
8	DDA	3689	3557	0.964
3	DA	3608	3533	0.979
8	DDA	3595	3528	0.981
4	DA	3416	3416	0.999
5	DA	3365	3360	0.998
8	DAA	3242	3087	0.952

the O atoms with Na^+ are called C to distinguish them from the hydrogen-bonded acceptors.

B. Frequencies. The frequencies for the different isomers are calculated using density functional theory (DFT) at the B3LYP/6-31+G** level. This basis set was identified as the best compromise between accuracy and computational cost in previous studies. The harmonic calculation and the DFT calculation with the limited basis set lead, for such a hydrogen-bonded system, to systematic errors in the calculation of the frequency spectrum. To correct for these deficiencies in a sensible way, we apply the following procedure. We calculate the frequencies for water clusters which contain most of the characteristic hydrogen-bonding patterns in the same approximation and derive the corrections by comparison with experiment. Here, we have chosen the cyclic structures of $n = 3$, 4, and 5, which are typical for the cooperative effects in hydrogen-bonding systems and which exhibit an increasing red shift of the 2-coordinated DA bonds.[25,37] In addition, the octamer cube is used, which exhibits the two characteristic 3-coordinated bonds of single DAA and double DDA donors.[25,38,39] The results are presented in Table 1. It is well-known that the harmonic approximation gives frequencies which are too high by 3−4% (too small of a red shift). This is reflected in the correction factors for the free OH stretch. The DFT calculations give, especially for cooperative effects, frequencies that are too low (too high red shifts).[40] This leads to a complete compensation of these effects and a correction factor of 1.0 in the frequency range of the water tetramer. This is not valid when competing processes are present, like in the 3-coordinated DDA and DAA bonds; in this case, again, too high frequencies result, which have to be corrected. We note that these corrections are far from being complete. Additional building blocks of larger water clusters and the interaction with the Na^+ and the electron are not considered. The reason is that for these features, no experimental results are available for comparison. We think that, despite these deficiencies, the results are much more reliable than those without these corrections.

IV. Comparison of Experiment and Calculations

On the basis of the preceding sections, we are now able to directly compare the corrected, calculated frequency spectrum of sampled representative isomers of one size with the experimental results. The quality of the experimental data, the approximations in the calculation, and the finite temperature of the clusters do not allow us to carry out the comparison for one selected isomer. Since we are mainly interested in the interpretation of the different peaks in the experimental spectrum, with emphasis on the interaction with the electron distribution, we average over the spectra of the four isomers with the lowest energy in the calculation. This also accounts implicitly for the finite temperature of the clusters, which we estimate, according to the experimental results for pure water clusters,[41] to be in the range of 60 K, a bit lower than the temperature of 300 K which was used in the MD calculation of this work.

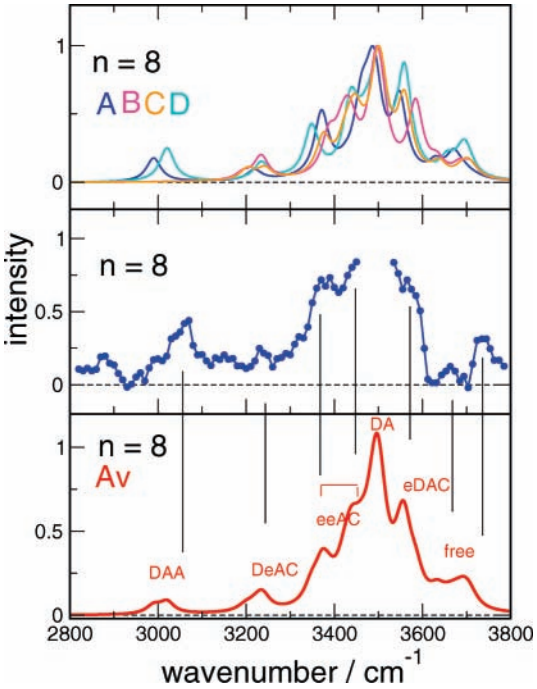

Figure 2. Comparison of measured (middle) and calculated (upper and lower panel) IR spectra of $Na(H_2O)_8$. The lower panel displays the spectrum of the average of the four lowest-energy isomers. The bonding type of the water molecules to which the OH mode belongs is indicated. The upper panel shows the results of the individual isomers in the marked colors.

The results for $n = 8$ are shown in Figure 2. The lower part exhibits the average spectrum of the four lowest-energy isomers, while the spectra of the single contributions are displayed in the upper part. The agreement between the measured and calculated average spectrum is surprisingly good for the position of the peaks. This is partly also valid for the general trend of the intensities. This is remarkable since the calculations reflect the pure vibrational absorption spectrum mainly based on the harmonic approximation, while the measurement is a complicated convolution of the vibrational excitation with the coupling to the delocalized electron distribution and the ionization process.

The analysis of the average spectrum in terms of contributions from single isomers is straightforward. They all peak around maxima and shoulders of the average spectrum with one exception. The peak at 3010 cm^{-1} is only observed in the spectra of the isomers 8A and 8D and not in those of isomers 8B and 8C. This leads to the lower intensity of this peak in the average spectrum in contrast to the measured data. This might be an indication that these isomers are present in the beam with lower probability. We show in Figures 3 and 4 two structures which are characteristic for the two groups. In both cases, the singly occupied molecular orbital (SOMO) of the delocalized electron dominates the picture. The cluster consists mainly of a network of 2-coordinated molecules of the DA and DC type, which are arranged around the Na^+ ion and the electron. The most remarkable features of the spectrum are the three direct interactions of H atoms with the electron, one with a double interaction, corresponding to the average peak positions at 3369 and 3443 cm^{-1}, and one with a single interaction, corresponding to the peak at 3563 cm^{-1}. The molecules to which these H atoms

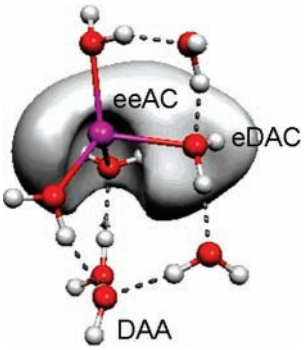

Figure 3. Calculated structure of the isomer 8D of $Na(H_2O)_8$. The configurations of the OH interactions with the electron distribution are indicated. The isodensity surface of the SOMO is plotted for 0.025 au.

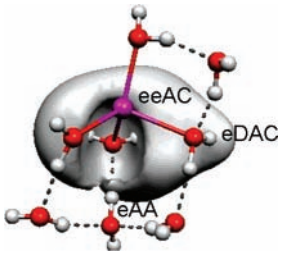

Figure 4. Calculated structure of the isomer 8B of $Na(H_2O)_8$. The configurations of the OH interactions with the electron distribution are indicated. Note the change from DAA (isomer 8D) to eAA. The isodensity surface of the SOMO is plotted for 0.025 au.

TABLE 2: Vibrational Transitions in cm^{-1} for the Four Lowest-Energy Isomers of $Na(H_2O)_8$

OH mode	A	B	C	D
eeAC	3370/3460	3387/3432	3374/3445	3347/3436
eDAC	3548	3584	3559	3559
eAA		3233	3201	
DC,DA	3424−3499	3444−3507	3420−3509	3444−3506
DAA	2990			3020
DeAC	3217	3193	3241	3233

TABLE 3: Number of OH-Stretch Modes of the Lowest-Energy Isomers of $Na(H_2O)_n$ Clusters

OH mode	8A	10A	16A	20A
free	6	4	8	9
ee..	1	1		1
e...	1	2	3	3
DA,DC	5	2	5	5
DAA,DAC	1	2	3	4
DDA,DDC		1	3	2
DDAA,DDAC		2	2	5

belong are both connected to the sodium ion in the configuration eeAC and eDAC. The results for the single line positions are presented in Table 2.

Continuing the interpretation of the $Na(H_2O)_8$ spectrum, the contributions of the five 2-coordinated DA or DC molecules are concentrated around the main peak of the calculated spectrum at 3490 cm^{-1}, which falls into the gap of the experimental spectrum. The manifestation of the free OH contributions at the least-shifted end (3700 cm^{-1}) and that of the DAA contribution at the most-red-shifted end (3020 cm^{-1}) of the spectrum is that which could be expected from what is known from pure water cluster spectra.[38,39] In two of the isomers, the DAA molecule is transferred to eAA molecules, which produces an additional interaction with the electron distribution. The extension of the electron cloud at the lower end, which causes this interaction, is clearly seen in Figure 4. Because of the coupling to the eeAC modes, the corresponding

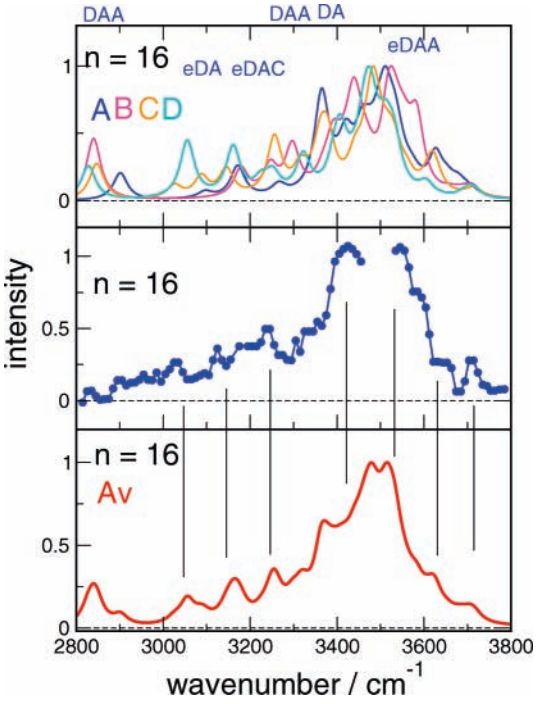

Figure 5. Comparison of measured (middle) and calculated (upper and lower panel) IR spectra of $Na(H_2O)_{16}$. The lower panel displays the spectrum of the average of the four lowest-energy isomers. The upper panel shows the results of the individual isomers in the marked colors. The bonding type of the water molecules with the main contribution is indicated. The first letter refers to the peak position.

line position is shifted to smaller wavenumbers close to the peak at 3220 cm^{-1}. This peak, which is present in all four isomers, originates from the hydrogen-bonded donor in the DeAC configuration, which in turn, is also connected to the electron. The general results for $n = 8$, which are listed in Table 2, show a remarkable agreement for all investigated isomers within 40 cm^{-1}. In this way, we get a clear picture of the band positions which interact with the electron distribution and which are caused by the hydrogen-bonded network.

For the larger clusters, the number of 3-coordinated single donor and double donor molecules increases at the expense of the 2-coordinated ones. This is shown in Table 3, in which the coordinations of the water molecules in the different clusters sizes are listed. A comparison of a spectrum for $n = 16$ is displayed in Figure 5. We have plotted the average spectrum of the four lowest-energy isomers in the lower panel and the contributions from the single isomers in the upper panel. The main features of the average spectrum are again reproduced by the calculation, aside from some deviations in the intensity around 3400 cm^{-1}. However, the origin of the peaks is not as easy to disentangle as that in the case of $n = 8$. Most of the peaks contain contributions from several isomers which consist of the interaction with the electron cloud of both H atoms of the type eeA and eeAC, and of one H atom of the types eA, eAA(eDA), and eDAA(eDAC). In addition, contributions from pure hydrogen-bonded molecules of the type DDA(DDC), DA(DC), DDAA(DDAC), and DAA(DAC) are observed with decreasing frequency all over the place. We have listed the configurations which mainly contribute to the peaks of the average spectrum in the upper part of Figure 5. Two characteristic structures are presented in Figures 6 and 7. The interactions with the electron are indicated in the figures. These are three single H atoms with one in the eDAC and two in the eDAA configuration for isomer 16B and one double H-atom

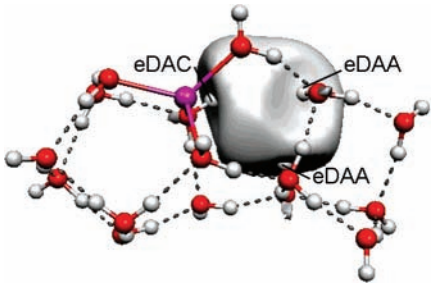

Figure 6. Calculated structure of the isomer 16B of $Na(H_2O)_{16}$. The configurations of the OH interactions with the electron distribution are indicated. The isodensity surface of the SOMO is plotted for 0.025 au.

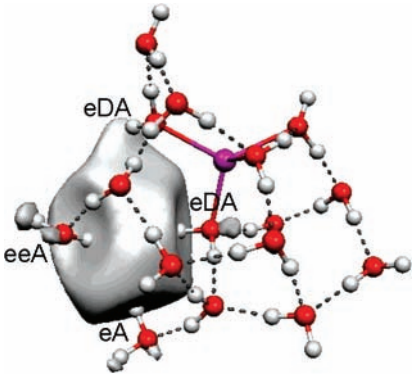

Figure 7. Calculated structure of the isomer 16C of $Na(H_2O)_{16}$. The configurations of the OH interactions with the electron distribution are indicated. The isodensity surface of the SOMO is plotted for 0.025 au.

TABLE 4: Vibrational Transitions in cm^{-1} for the Interaction of H Atoms with the Solvated Electron in $Na(H_2O)_{16}$ Clusters

OH mode	wavenumber	isomer	comment
eeAC	3423/3502	A	
eeA	3378/3623	C	weak[a]
eDAC,eDAA	3626	A	weak [a]
	3533	A	weak[a]
	3516	B	D coup[b]
	3435	B	D coup[b]
	3295	B	D coup[b]
	3160	D	strong[a]
eDA	3620	C	weak[a]
	3359	C	
	3320	D	
	3054	D	strong[a]
eA	3482	C	

[a] Weak or strong electron intensity. [b] Coupling to the donor D in the same molecule.

interaction eeA and three single H-atom interactions of the type eA and eDA for isomer 16C.

The results for the line positions of the interaction with the electron distribution are presented in Table 4. The comparison of these results with the clear-cut values obtained for $n = 8$, which are 3563 cm^{-1} for eDAC (eDAA) and 3217 cm^{-1} for eDC (eDA), reveals a couple of interesting features. In both cases, the values for $n = 16$ are spread from 3626 to 3160 cm^{-1} and from 3620 to 3054 cm^{-1}, respectively. We found two different reasons for this behavior. (a) The values around 3620 cm^{-1} indicate small shifts. The inspection of the electron distribution reveals that, in these cases, the density and thus the interaction is weaker. This can be nicely observed in Figure 7 in the eeA on the left-hand side and in the eDA configurations in the top position. The values around 3100 cm^{-1} are traced back to a stronger density. This result offers an interesting method to probe the strength of the interaction with the electron distribution by IR spectroscopy. (b) Aside from the weak and strong lines, the results for the eDAC (eDAA) configurations exhibit an additional effect. Apparently, the increasing number of molecules and the additional connection to the network leads to a further coupling. A closer inspection shows that the peak intensities at 3516, 3435, and 3295 cm^{-1} originate from the fact that the motion of the H atoms in the direction of the electron is coupled to that of their respective donor H atoms in the same molecule which are connected to the hydrogen-bonded network. The corresponding peaks of this combined motion are found at 3470, 3389, and 3444 cm^{-1} with lower intensity. Finally, we note that the eA configuration is less red shifted in comparison with the eAC configuration of $n = 8$, a result which is in line with a model calculation for small metal−water clusters.[42]

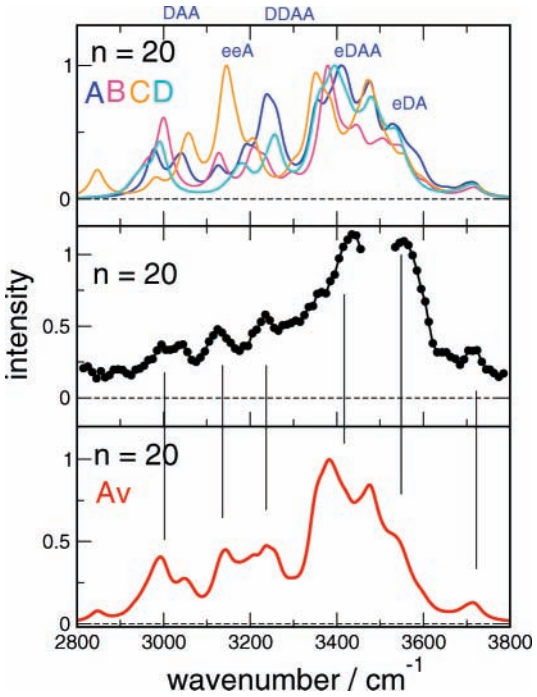

Figure 8. Comparison of measured (upper) and calculated (upper and lower panel) IR spectra of $Na(H_2O)_{20}$. The lower panel displays the spectrum of the average of the four lowest-energy isomers. The upper panel shows the results of the individual isomers in the marked colors. The bonding types of the water molecules with the main contribution are indicated. The first letter refers to the peak position.

The other two investigated cluster sizes $n = 10$ and 20 resemble the two examples already presented. The cluster with $n = 10$ water molecules is only a little bit larger than the presented octamer. The four interactions with the electron manifest themselves in peaks in the spectrum with similar positions as those found for the octamer. In one case, we find a blue-shifted position which results from a weaker intensity of the electron cloud. The results for $n = 20$ are shown in Figure 8. The comparison with the spectrum based on the four lowest-energy isomers exhibits a satisfying agreement, with the exception of the range close to 3400 cm^{-1}. Here, the actual position of the main peak differs by 50 cm^{-1}, which could also be a problem of intensity. This result could not be improved by adding the spectra of up to five more isomers to the spectrum. It appears that at this cluster size, the calculation of the IR spectrum starts to become difficult.

Nevertheless, the comparison of the frequencies of the different isomers, which indicates the interaction with the electron distribution, exhibits consistent results. They are presented in Table 5. The double H-atom interactions of the

TABLE 5: Vibrational Transitions in cm^{-1} for the Interaction of H Atoms with the Solvated Electron in Na$(H_2O)_{20}$Clusters

OH mode	wavenumber	isomer	comment
eeA	3188/3586	A	
	3206/3572	B	
	3173/3574	C	
	3168/3618	D	
eDAC,eDAA	3413	A	
	3396	D	
	3389	B	
	3385	B	
	3375	A	
eDA	3575	A	weak[a]
	3525	A	D coup[b]
	3509	D	D coup[b]
	3380	B	
	3062	C	strong[a]

[a] Weak or strong electron intensity. [b] Coupling to the donor D in the same molecule.

eeA type are all in the range of 3183/3587 cm^{-1}. Surprisingly, the single H-atom interactions of the eDAA(eDAC) type occur around 3392 cm^{-1} without any large spread. Those of the eDA type are again spread from 3575 to 3062 cm^{-1}. The first and the last ones are caused by the weak and strong intensity of the electron cloud. Two other values in the middle are traced back to the coupling of the H atom interacting with the electron and the donor, similar to the result found for the eDAA(eDAC) configurations of $n = 16$. The electron interactions are shown for the lowest-energy isomer 20A in Figure 9. When we analyze the peaks in the average spectrum of Figure 8 in terms of the origin in the upper part of the figure, we see that the main peak between 3400 and 3600 cm^{-1} is essentially composed of contributions from the electron interaction. The peak with the largest red shift at 2977 cm^{-1} is mainly caused by DAA molecules, while the next two peaks at 3130 and 3236 cm^{-1} are due to electron interactions of the eeA type and 4-coordinated DDAA molecules, respectively. We note that, in both cases, contributions from the hydrogen-bonded network at higher frequencies and from the electron interaction at lower frequencies are also observed. Apparently, coupling to many other modes occurs, and the clear signature of the interaction with the electron distributions disappears at this clusters size.

V. Discussion

The results of all of the interactions with the electron are summarized in Table 6. The positions of the single H-atom motifs of the eDAC(eDAA) type are found at 3563 and 3538 cm^{-1} for $n = 8$ and 10, respectively, and at 3392 cm^{-1} for $n = 20$. The results for $n = 16$ vary from 3626 to 3160 cm^{-1}. The eDA(eAA) motif exhibits a reversed behavior. It starts at smaller values of 3217 cm^{-1} for $n = 8$ and increases to values of 3340 and 3410 cm^{-1} for $n = 16$ and 20, respectively. In both cases, strong variations occur. They are traced back to changes in the electron density at the point of interaction and the coupling caused by the strong interaction of the H atom bound to the electron with the corresponding donor D in the same molecule. Apparently, the larger clusters lead to a larger variation of the electron density, which also blurs the differences between the eDAC and eDA motifs which are clearly observed for $n = 8$.

The double interaction of the molecule with the electron in the eeAC configuration is best observed for $n = 8$. The doublet which occurs at 3369/3443 cm^{-1} has a slight separation and is shifted in the position compared to that observed in recent experiments of the vibrational spectroscopy of water anions

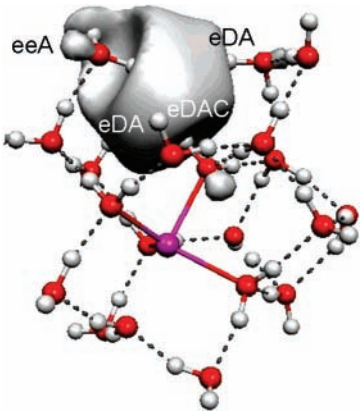

Figure 9. Calculated structure of the lowest-energy isomer A of Na$(H_2O)_{20}$. The configurations of the OH interactions with the electron distribution are indicated. The isodensity surface of the SOMO is plotted for 0.025 au.

TABLE 6: Vibrational Transitions in cm^{-1} for the Interaction of H Atoms with the Solvated Electron in Na$(H_2O)_n$ Clusters Averaged over All Contributions of the Four Lowest-Energy Isomers

OH mode	8	10	16	20
eeAC	3369/3443	3358/3546	3423/3502	
eeA		3390/3621	3378/3623	3183/3587
eDAC,eDAA	3563	3538	3428[a]	3392
eDA,eAA	3217		3340[b]	3410[c]

[a] Spread 3626−3160. [b] Spread 3572−3062. [c] Spread 3620−3054.

$(H_2O)_{20}^-$ carried out by the group of Johnson.[15] In their argon-mediated predissociation and photodetachment data, they observed the binding motif of a single water molecule through a double H bond to the electron cloud (eeAA in our nomenclature), which led to a pronounced double peak at 3260 and 3400 cm^{-1} in the OH-stretch spectra of the clusters for $n = 6-8$. The differences with the present experiment may be traced back to the presence of the Na^+ in this work. The larger clusters exhibit mainly weak features which are, in addition, split by larger amounts. The eeA feature exhibits a more consistent, picture with a large splitting which is caused by one weak coupling close to 3600 cm^{-1}.

We note that the simple picture presented in the first publication of the data, in which the peak around 3400 cm^{-1} was responsible for the coupling to the electron, does not hold anymore.[22] Both peaks close to 3400 and 3550 cm^{-1} can be traced back to the interaction with the electron, with a preference of the single H-atom interaction for the latter one. In addition, also some smaller peaks at lower frequencies originate from this interaction. With increasing size, these features mix with the usual interactions of the typical hydrogen-bonded network and more or less disappear at $n = 20$. For $n = 16$ and 20, in addition, different isomers also contribute to the measured spectrum at different places so that it is difficult to trace single spectral features back to a special structural behavior.

The results obtained so far allow us to derive some conclusion about the structure of these small sodium-doped water clusters and also on the position of the electron. The octamer which is displayed in Figures 3 and 4 mainly consists of a 2-coordinated hydrogen-bonded network arranged around the electron cloud by four- and five-membered rings. The Na^+ ion takes the position of one of the water molecules and replaces the hydrogen-bonded donor connected to the O atom (C configuration). For $n = 16$, we have again plotted two characteristic isomers in Figures 6 and 7. One is quite symmetric and, with

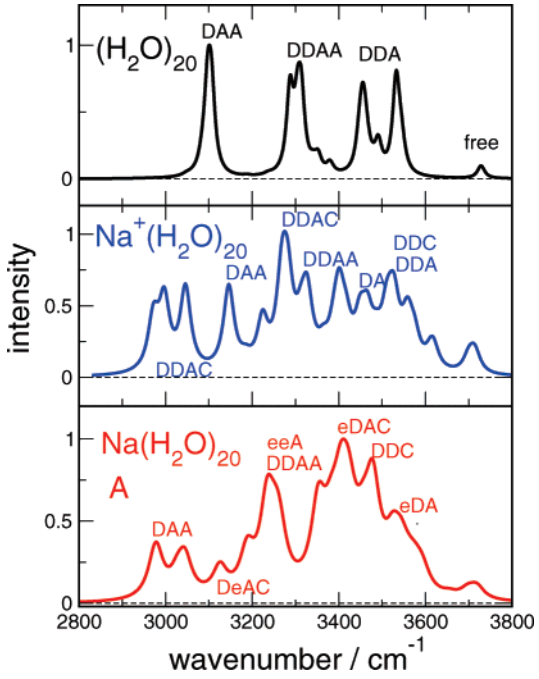

Figure 10. Comparison of calculated IR spectra of the minimum-energy configurations of pure $(H_2O)_{20}$ clusters,[26] of $Na^+(H_2O)_{20}$ clusters,[27] and of $Na(H_2O)_{20}$ clusters of this work. The bonding type of the water molecules to which the OH mode belongs is indicated. The first letter refers to the peak position.

its edge-sharing pentagonal prisms at the left-hand side, resembles the minimum structure of the pure $(H_2O)_{20}$ clusters,[26] but with single five- and four-membered rings attached to it. The other is of a more spherical shape with an irregular arrangement of the different rings. Again, the Na^+ ion is integrated in the network like a water molecule. All of the other isomers belong to one of these groups. This behavior is different from the calculated structures of $Na^+(H_2O)_{20}$ clusters.[27] Here, the Na^+ forms a sort of center, though not in a symmetric position, which is surrounded by six water molecules. The result for $n = 20$ in Figure 9 resembles very much the more spherical shape of $n = 16$ in Figure 7. The other isomers are either of this shape or somewhat elongated, similar to the one of $n = 16$ in Figure 6. However, none of them exhibits one of the very symmetric structures observed for pure water clusters.[26] In all cases, the electron distribution is at the surface of the clusters in the sort of arrangement which is displayed in Figure 9. The electron distribution is partly surrounded by water molecules but still at the surface. We note that this general result of a surface electron is in line with a couple of the other experimental and theoretical results found in this size range for negatively charged water clusters.[16,19]

The results which were obtained in the last sections enable us to compare them with calculations which are available for the pure water $(H_2O)_{20}$ cluster and the cation cluster $Na^+(H_2O)_{20}$. Since both are calculations based on the minimum configuration of the clusters, we also use the minimum configuration of $Na(H_2O)_{20}$ for the comparison. This comparison is shown in Figure 10. The simplest spectrum is definitely that of the pure water cluster, which consists of three edge-sharing pentagonal prisms in its minimum configuration.[26] This system contains six free OH groups, six DDA, six DAA, and eight DDAA molecules. Consequently, the spectrum exhibits four groups which are clearly separated from each other, the free OH groups, the split 3-coordinated double donor DDA, the 4-coordinated DDAA, and the 3-coordinated DAA single donor OH groups,

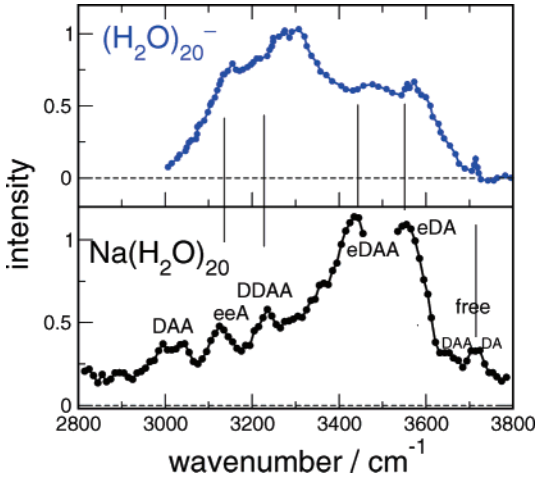

Figure 11. Comparison of measured IR spectra of $(H_2O)_{20}^-$ clusters[16] and of $Na(H_2O)_{20}$ clusters of this work. The bonding-type terms are taken from the calculations of the average spectrum of Figure 8.

which exhibit the largest shifts. The two doped clusters with a more random arrangement of the hydrogen-bonded network clearly show a more complicated structure. The Na^+ containing clusters exhibit, aside from the additional 2-coordinated DA configurations, shifts in about the same frequency range. What is interesting is the behavior of those molecules which are connected to the Na^+ ion, in our nomenclature C. They are again in the same frequency range as their counterparts in a pure hydrogen-bonded network, aside from the doublet in the 3050 cm^{-1} region. In contrast, the $Na(H_2O)_{20}$ cluster, which besides the Na^+, also contains the solvated electron distribution, shows a different behavior. The main peaks exhibit, in addition to the expected contributions from the 4- and 3-coordinated molecules, fingerprints of the interaction with the electron. The large red-shifted pattern in the $Na^+(H_2O)_{20}$ cluster, originating from the coupling to Na^+, is also observed in the neutral cluster. However, here, they can be traced back to DAA molecules.

A probably even more interesting comparison is that with the measured spectrum of the negatively charged water cluster $(H_2O)_{20}^-$, which is displayed in Figure 11.[16] Here, both clusters contain the electron distribution but with and without the counterion Na^+ present. Both spectra share the general appearance with no spectacular peak structure. Apparently, the number of oscillators is already quite large so that, in addition to the possible isomers, also the coupling of the oscillators comes into play. The two spectra have their peak intensities in completely different frequency ranges. The peaks of the $Na(H_2O)_{20}$ spectrum occur between 3400 and 3600 cm^{-1}. They are mainly caused by the interaction of the H atoms of the water molecules with the electron distribution. The peak at 3416 cm^{-1} also contains contributions from 4-coordinated molecules. The peak intensity of the $(H_2O)_{20}^-$ cluster ion is found in the range of 3100 to 3300 cm^{-1}. The very pronounced binding motif of the eeAA type observed for small cluster sizes is assumed to be shifted into this range and is weakened by the coupling to other modes. The fingerprints of the $Na(H_2O)_{20}$ spectrum in this frequency range show similar behavior. Aside from the typical contributions of 4-coordinated molecules (DDAA, DDAC), we still observe a direct interaction of the electrons (eeA) and a peak caused by the 3-coordinated single donor DAA. We finally note that in the case of the $Na(H_2O)_{20}$ cluster, the contributions to the free OH modes come from DA and DAA molecules, with a larger intensity of the first one. The spectrum of $(H_2O)_{20}^-$ exhibits only one peak.

VI. Conclusions

We have compared the measured vibrational OH-stretch spectra of size-selected $Na(H_2O)_n$ clusters for $n = 8$, 10, 16, and 20 with calculations based on density functional theory. In a first step, ab initio molecular dynamics are employed to sample representative structures at finite temperature. In a second step, these structures are used for structural optimization, applying the Gaussian program. The resulting harmonic frequencies are corrected by comparing calculations for pure water clusters within the same basis set with the corresponding experimental results. The experimental spectra of $Na(H_2O)_n$ are all dominated by peaks around 3430 and 3550 cm^{-1}. The comparison with the calculated and corrected spectra definitely shows that they mainly originate from the interaction of the H atoms of the OH group with the solvated electron distribution.

The interaction of both H atoms with the electron is best observed for $n = 8$ in the eeAC configuration, with a doublet at 3369/3443 cm^{-1}. In the larger clusters, these features have larger splitting and start to be buried under intensity peaks of other origins. The fingerprint of a single electron is size dependent. For the eDAA (eDCA) configuration, it starts at 3563 for $n = 8$ and at 3538 cm^{-1} for $n = 10$ and ends at 3392 cm^{-1} for $n = 20$. For the eAA (eDA) configuration, it is found at 3217 cm^{-1} for $n = 8$ and at 3410 cm^{-1} for $n = 20$. The values for $n = 16$ contain a range of frequencies between 3620 and 3054 cm^{-1}, which are caused by different electron densities and special couplings to other OH modes.

Aside from the interaction with the electron distribution, we also observe the typical motifs of a hydrogen-bonded network, namely, with decreasing wavenumbers and increasing strength of the hydrogen bond, the free, the 3-coordinated double donor DDA and DDC, the 2-coordinated DA and DC, the 4-coordinated DDAA and DDAC, and finally the 3-coordinated DAA molecules. While the DA and DAA contributions are separated from each other and from the electron contributions for $n = 8$, this separation is lost for the larger clusters, and we observe a mixture with the electron interactions. The free OH-stretch consists, in contrast to the results of pure water clusters, of two peaks. The one with the larger intensity originates from DA molecule, and the other one is from DAA molecules.

All of the sodium-doped water clusters exhibit structures with a localized electron distribution which is situated at the surface. The hydrogen-bonded networks are attached to this distribution. In the case of $n = 8$, it predominantly consists of 2-coordinated DA molecules. For the larger clusters, more and more 3- and 4-coordinated molecules come into play. For $n = 16$ and 20, they are arranged in elongated or spherical shapes. However, also for $n = 20$, they never reach any of the very symmetric configurations which were found for pure water clusters.

Acknowledgment. We thank Dr. Christof Steinbach for the measurement and the evaluation of the IR spectra and Professor Martin Suhm for valuable hints and support of the calculation of the corrections. We are grateful to Dr. Franziska Schulz for providing details of their calculations of sodium ion water clusters.

References and Notes

(1) Shkrob, I. A. *J. Phys. Chem. A* **2006**, *110*, 3967.
(2) Copeland, D. A.; Kestner, N. R.; Jortner, J. *J. Chem. Phys.* **1970**, *53*, 1189.
(3) Abramczyk, H.; Kroh, J. *Radiat. Phys. Chem.* **1994**, *43*, 291.
(4) Sprik, M.; Impey, R. W.; Klein, M. L. *Phys. Rev. Lett.* **1986**, *56*, 2326.
(5) Marchi, M.; Sprik, M.; Klein, M. L. *J. Phys.: Condens. Matter* **1990**, *2*, 5833.
(6) Deng, Z.; Martyna, G. J.; Klein, M. L. *J. Chem. Phys.* **1994**, *100*, 7590.
(7) Boero, M.; Parrinello, M.; Terekura, K.; Ikeshoji, T.; Liew, C. C. *Phys. Rev. Lett.* **2003**, *90*, 226403-1.
(8) Rossky, P. J.; Schnitker, J. *J. Phys. Chem.* **1988**, *92*, 4277.
(9) Barnett, R. N.; Landman, U.; Cleveland, C. L.; Kestner, N. R.; Jortner, J. *Chem. Phys. Lett.* **1988**, *148*, 249.
(10) Marchi, M.; Sprik, M.; Klein, M. L. *J. Chem. Phys.* **1988**, *89*, 4918.
(11) Makov, G.; Nitzan, A. *J. Phys. Chem.* **1994**, *98*, 3459.
(12) *Clusters of Atoms and Molecules*; Haberland, H., Ed.; Springer: Berlin, Germany, 1994.
(13) Haberland, H.; Langosch, H.; Schindler, H. G.; Worsnop, D. R. *J. Phys. Chem.* **1984**, *88*, 3903.
(14) Sarkas, H. W.; Arnold, S. T.; Eaton, J. G.; Lee, G. H.; Bowen, K. H. *J. Chem. Phys.* **2002**, *116*, 5731.
(15) Hammer, N. I.; Shin, J. W.; Headrick, J. M.; Diken, E. G.; Roscioli, J. R.; Weddle, G. H.; Johnson, M. A. *Science* **2004**, *306*, 675.
(16) Hammer, N. I.; Roscioli, J. R.; Bopp, J. C.; Headrick, J. M.; Johnson, M. A. *J. Chem. Phys.* **2005**, *123*, 123.
(17) Verlet, J. R. R.; Bragg, A. E.; Kammrath, A.; Cheshnovsky, O.; Neumark, D. M. *Science* **2005**, *307*, 93.
(18) Paik, D. H.; Lee, I. R.; Yang, D. S.; Baskin, J. S.; Zewail, A. H. *Science* **2004**, *306*, 672.
(19) Turi, L.; Sheu, W. S.; Rossky, P. J. *Science* **2005**, *309*, 914.
(20) Schulz, C. P.; Haugstätter, R.; Tittes, H.-U.; Hertel, I. V. *Phys. Rev. Lett.* **1986**, *57*, 1703.
(21) Steinbach, C.; Buck, U. *J. Chem. Phys.* **2005**, *122*, 134301.
(22) Steinbach, C.; Buck, U. *J. Phys. Chem. A* **2006**, *110*, 3128.
(23) Salter, T. E.; Mikhailov, V. A.; Evans, C. J.; Ellis, A. M. *J. Chem. Phys.* **2006**, *125*, 034302.
(24) Gao, B.; Liu, Z. F. *J. Chem. Phys.* **2007**, *126*, 084501.
(25) Buck, U.; Huisken, F. *Chem. Rev.* **2000**, *100*, 3863.
(26) Fanourgakis, G. S.; Apra, E.; de Jong, W. A.; Xantheas, S. S. *J. Chem. Phys.* **2005**, *122*, 134304.
(27) Schulz, F.; Hartke, B. *Phys. Chem. Chem. Phys.* **2004**, *5*, 5021.
(28) Weinheimer, C. J.; Lisy, J. M. *J. Chem. Phys.* **1996**, *105*, 2938.
(29) Schütte, S.; Buck, U. *Int. J. Mass Spectrom.* **2002**, *220*, 183.
(30) Huisken, F.; Kulcke, A.; Voelkel, D.; Laush, C.; Lisy, J. M. *Appl. Phys. Lett.* **1993**, *62*, 805.
(31) Buck, U.; Ettischer, I. *J. Chem. Phys.* **1998**, *108*, 33.
(32) Kresse, G.; Hafner, J. *Phys. Rev. B* **1993**, *47*, 558.
(33) Kresse, G.; Hafner, J. *Phys. Rev. B* **1994**, *49*, 14251.
(34) Kresse, G.; Furthmüller, J. *Phys. Rev. B* **1996**, *54*, 11169.
(35) Kresse, G.; Furthmüller, J. *Comput. Mater. Sci.* **1996**, *6*, 15.
(36) Frisch, M. J.; Trucks, G. W.; Schlegel, H. B.; Scuseria, G. E.; Robb, M. A.; Cheeseman, J. R.; Montgomery, J. A., Jr.; Vreven, T.; Kudin, K. N.; Burant, J. C.; Millam, J. M.; Iyengar, S. S.; Tomasi, J.; Barone, V.; Mennucci, B.; Cossi, M.; Scalmani, G.; Rega, N.; Petersson, G. A.; Nakatsuji, H.; Hada, M.; Ehara, M.; Toyota, K.; Fukuda, R.; Hasegawa, J.; Ishida, M.; Nakajima, T.; Honda, Y.; Kitao, O.; Nakai, H.; Klene, M.; Li, X.; Knox, J. E.; Hratchian, H. P.; Cross, J. B.; Bakken, V.; Adamo, C.; Jaramillo, J.; Gomperts, R.; Stratmann, R. E.; Yazyev, O.; Austin, A. J.; Cammi, R.; Pomelli, C.; Ochterski, J. W.; Ayala, P. Y.; Morokuma, K.; Voth, G. A.; Salvador, P.; Dannenberg, J. J.; Zakrzewski, V. G.; Dapprich, S.; Daniels, A. D.; Strain, M. C.; Farkas, O.; Malick, D. K.; Rabuck, A. D.; Raghavachari, K.; Foresman, J. B.; Ortiz, J. V.; Cui, Q.; Baboul, A. G.; Clifford, S.; Cioslowski, J.; Stefanov, B. B.; Liu, G.; Liashenko, A.; Piskorz, P.; Komaromi, I.; Martin, R. L.; Fox, D. J.; Keith, T.; Al-Laham, M. A.; Peng, C. Y.; Nanayakkara, A.; Challacombe, M.; Gill, P. M. W.; Johnson, B.; Chen, W.; Wong, M. W.; Gonzalez, C.; Pople, J. A. *Gaussian 03*, revision A.01; Gaussian, Inc.: Pittsburgh, PA, 2003.
(37) Huisken, F.; Kaloudis, M.; Kulcke, A. *J. Chem. Phys.* **1996**, 104, 17.
(38) Sadlej, J.; Buch, V.; Kazimirski, J.; Buck, U. *J. Phys. Chem. A* **1999**, *103*, 4933.
(39) Buck, U.; Ettischer, I.; Melzer, M.; Buch, V.; Sadlej, J. *Phys. Rev. Lett.* **1998**, *80*, 2578.
(40) Maerker, C.; Schleyer, P. v. R.; Liedl, K. R.; Ha, T.-K.; Quack, M.; Suhm, M. *J. Comput. Chem.* **1997**, *18*, 1695.
(41) Brudermann, J.; Buck, U.; Buch, V. *J. Phys. Chem. A* **2002**, *106*, 453.
(42) Tsurusawa, T.; Iwata, S. *J. Chem. Phys.* **2000**, *112*, 5705.